

COUPLING POWER FLOW FROM THE MERCURY MIVA INTO A ROD-PINCH DIODE *

J.W. Schumer^a, R.J. Allen, R.J. Comisso, and P.F. Ottinger

Plasma Physics Division, Naval Research Laboratory, Washington, DC 20375

Abstract

The Mercury machine at NRL, formerly known as KALIF-HELIA [1] at Forschungszentrum Karlsruhe (Germany), is a magnetically-insulated inductive voltage adder (MIVA), nominally delivering a 50-ns, 6-MV, 360-kA, 2.2-TW power pulse into a 16-Ω load [2,3,4]. Mercury is capable of operating in both positive and negative polarities with little penalty in pulsed-power output. Polarity reversal is achieved by insertion of the tapered center conductor into the opposite end of the MIVA. In this work, particle-in-cell (PIC) simulations [5,6] are used to investigate the power flow within the magnetically-insulated transmission line (MITL) in both polarities. Of particular importance is the efficiency of operation when an over-matched 50-Ω rod-pinch-diode load is couple to the MITL, operated in either positive [7] or negative [8] polarity. Such a diode is used for radiographic applications because of the small, high brightness radiation source produced by the electron pinch at the end of the diode's anode rod [9]. Simple positive and negative polarity diode geometries are studied in preparation for initial rod-pinch diode experiments on Mercury.

I. INTRODUCTION

Mercury is a 50-ns, 6-MV, 360-kA accelerator with a magnetically-insulated inductive-voltage-adder (MIVA) architecture, and can be operated in either positive or negative polarity [1,2]. Because voltage is added in vacuum along a magnetically-insulated transmission line (MITL) from six voltage adder cells, understanding electrical power flow and subsequent coupling to various loads requires the application of circuit modeling [3] utilizing MITL theory [4], both supported by numerical simulations. In this work, MAGIC [5] and LSP [6] particle-in-cell (PIC) simulations are performed to investigate the electron power-flow within the MITL, driven by the Mercury MIVA in both positive and negative polarities (see Figure 1). One goal is to provide insight into the development of appropriate, physics-based MITL circuit-element models for the NRL

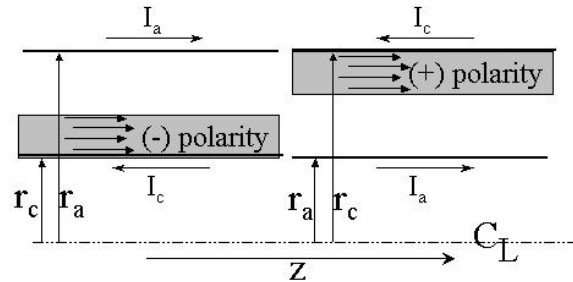


Figure 1. Schematic of MITL flow in negative (-) and positive (+) polarity.

transmission line code BERTHA [10] by properly treating power flow and load coupling in the vacuum section of Mercury. Another is to understand how to shed MITL current and design more efficient diode loads.

The fundamental understanding of MITL flow is derived from a pressure balance argument when space charge limited (SCL) emission occurs at the cathode [4]. This assumption of SCL emission implies that the cathode is turned-on and that there is sufficient space charge in the gap to drive the electric field to zero at the cathode surface. The model allows for the possibility of additional electron emission at any point along the MITL if there is not enough space charge in the gap or, conversely, electron current loss to the anode or re-trapping to the cathode if there is too much space charge in the gap. The electrons are emitted from the cathode with zero energy (and, hence, at zero pressure), and the electron pressure at the anode is negligible compared to the electromagnetic field pressure. No ion emission from the MITL anode is allowed.

The general form for the flow impedance Z_f is

$$Z_f = \frac{V}{\sqrt{I_a^2 - I_c^2}}, \quad (1)$$

where V is the voltage across the anode-cathode gap in the MITL, I_a is the current flowing in the anode, I_c is the current flowing in the cathode, and $I_a - I_c$ is the current flowing in the vacuum as an electron flow layer. This definition for Z_f is independent of the distribution of space charge in the AK gap. For the case where the space charge density is uniform across the sheath,

* Work supported by US DOE (through SNL, LANL, and LLNL), NRL, and DTRA

^a Email: schumer@nrl.navy.mil

Report Documentation Page

Form Approved
OMB No. 0704-0188

Public reporting burden for the collection of information is estimated to average 1 hour per response, including the time for reviewing instructions, searching existing data sources, gathering and maintaining the data needed, and completing and reviewing the collection of information. Send comments regarding this burden estimate or any other aspect of this collection of information, including suggestions for reducing this burden, to Washington Headquarters Services, Directorate for Information Operations and Reports, 1215 Jefferson Davis Highway, Suite 1204, Arlington VA 22202-4302. Respondents should be aware that notwithstanding any other provision of law, no person shall be subject to a penalty for failing to comply with a collection of information if it does not display a currently valid OMB control number.

1. REPORT DATE JUN 2003	2. REPORT TYPE N/A	3. DATES COVERED -	
4. TITLE AND SUBTITLE Coupling Power Flow From The Mercury Miva Into A Rod-Pinch Diode		5a. CONTRACT NUMBER	
		5b. GRANT NUMBER	
		5c. PROGRAM ELEMENT NUMBER	
6. AUTHOR(S)		5d. PROJECT NUMBER	
		5e. TASK NUMBER	
		5f. WORK UNIT NUMBER	
7. PERFORMING ORGANIZATION NAME(S) AND ADDRESS(ES) Plasma Physics Division, Naval Research Laboratory, Washington, DC 20375		8. PERFORMING ORGANIZATION REPORT NUMBER	
9. SPONSORING/MONITORING AGENCY NAME(S) AND ADDRESS(ES)		10. SPONSOR/MONITOR'S ACRONYM(S)	
		11. SPONSOR/MONITOR'S REPORT NUMBER(S)	
12. DISTRIBUTION/AVAILABILITY STATEMENT Approved for public release, distribution unlimited			
13. SUPPLEMENTARY NOTES See also ADM002371. 2013 IEEE Pulsed Power Conference, Digest of Technical Papers 1976-2013, and Abstracts of the 2013 IEEE International Conference on Plasma Science. IEEE International Pulsed Power Conference (19th). Held in San Francisco, CA on 16-21 June 2013. U.S. Government or Federal Purpose Rights License., The original document contains color images.			
14. ABSTRACT The Mercury machine at NRL, formerly known as KALIF-HELIA [1] at Forschungszentrum Karlsruhe (Germany), is a magnetically-insulated inductive voltage adder (MIVA), nominally delivering a 50-ns, 6-MV, 360-kA, 2.2-TW power pulse into a 16-\bar{U} load [2,3,4]. Mercury is capable of operating in both positive and negative polarities with little penalty in pulsed-power output. Polarity reversal is achieved by insertion of the tapered center conductor into the opposite end of the MIVA. In this work, particle-in-cell (PIC) simulations [5,6] are used to investigate the power flow within the magnetically-insulated transmission line (MITL) in both polarities. Of particular importance is the efficiency of operation when an over-matched 50-\bar{U} rod-pinch-diode load is couple to the MITL, operated in either positive [7] or negative [8] polarity. Such a diode is used for radiographic applications because of the small, high brightness radiation source produced by the electron pinch at the end of the diodes anode rod [9]. Simple positive and negative polarity diode geometries are studied in preparation for initial rod-pinch diode experiments on Mercury.			
15. SUBJECT TERMS			
16. SECURITY CLASSIFICATION OF:			17. LIMITATION OF ABSTRACT SAR
a. REPORT unclassified	b. ABSTRACT unclassified	c. THIS PAGE unclassified	
			18. NUMBER OF PAGES 4
			19a. NAME OF RESPONSIBLE PERSON

$$V = Z_0 \left(I_a^2 - I_c^2 \right)^{1/2} - \frac{mc^2}{2e} \frac{I_a^2 - I_c^2}{I_c^2}, \quad (2)$$

where m and e are the mass and charge of an electron and c is the speed of light. The last term is the space charge correction. This voltage formula agrees with measurements in PIC simulations to within 3% in negative polarity and to within 30% in positive polarity. Polarity dependence of the electron flow is discussed further below.

II. OPEN-CIRCUIT LOAD DRIVEN IN NEGATIVE OR POSITIVE POLARITY

Numerical simulations of the Mercury MIVA were performed using LSP [6] in 2D cylindrical geometry. The inner and outer radii of the MITL are identical to those on the machine; however, the detailed geometry of the six radial feed-gaps was ignored in this analysis. In Table 1, the radii immediately downstream of each cell and the respective vacuum impedances of these sections are listed.

Table 1. Summary of vacuum and flow impedances, just downstream of each adder section. The respective inner and outer radii for each section are also listed. Three different flow impedances were obtained for the three different self-limited simulations for (a) negative polarity, (b) negative polarity with cell-emission, and (c) positive polarity.

Cell#	R_{inner} [cm]	R_{outer} [cm]	Z_0 [Ω]	(-) pol Z_f [Ω]	(-) pol ee Z_f [Ω]	(+) pol Z_f [Ω]
1	16.6	190.5	8.26	7.40	7.65	5.89
2	15.05	190.5	14.14	12.97	12.45	8.11
3	13.9	190.5	18.91	18.76	16.63	11.09
4	13.0	190.5	22.93	21.30	20.22	14.05
5	12.2	190.5	26.74	24.95	23.68	16.09
6	11.55	190.5	30.02	26.24	25.23	18.50

Trapezoidal voltage waveforms rising to 1.0 MV with a 40-ns FWHM were applied to each radial feed-gap. Note that this does not represent Mercury at full power. To provide speed-of-light synchronization between the feed-gaps, a 2-ns differential timing was used (i.e. there is a 2 ns delay between the inputs of the adjacent feed-gaps).

Electron emission in the simulations is initiated when the electric field exceeds 250 kV/cm and it is controlled by a standard space-charge-limiting model, maintaining a zero normal electric field on the surface. No ions were permitted in these simulations. In these simulations, “polarity” refers to the relative potential of the center conductor with respect to ground, or outer conductor.

In Fig. 2, electron positions within the MIVA at $t = 50$ ns are shown for three different simulations with an open-circuit load: (a) negative polarity, (b) negative

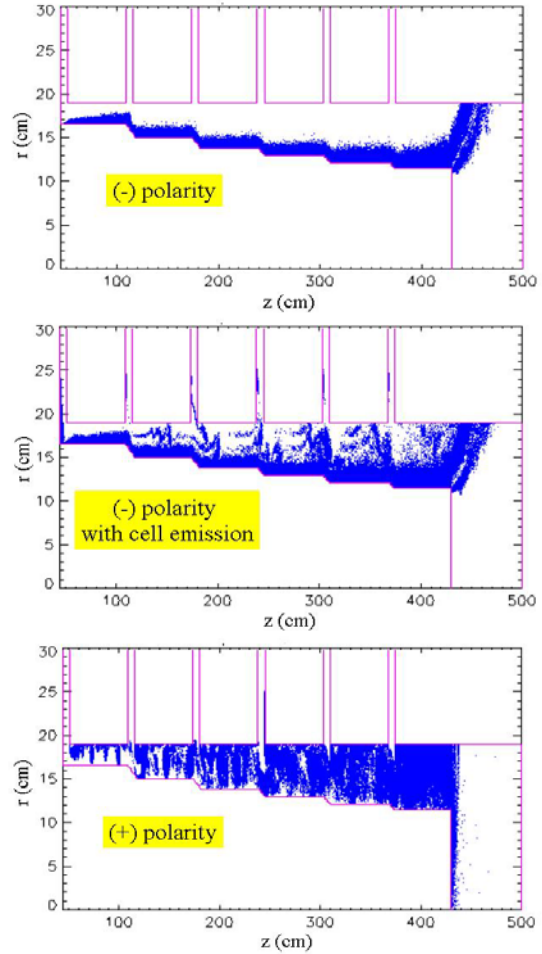


Figure 2. Snapshot of self-limited electron powerflow in Mercury MIVA with an open-circuit load, for three cases: (a) negative polarity, (b) negative polarity allowing for electron-emission from the cells, and (c) positive polarity.

polarity with electron emission from the cell adder sections, and (c) positive polarity. One should note two important points. First, with an open-circuit diode load, these cases represent the highest voltage operation expected with the current center conductor geometry. Second, allowing of cell-emission in negative polarity results in layered flow, which is both expected and seen in positive polarity. This layered flow lowers the flow impedance by distributing the space charge across the vacuum gap. In addition, electrons in each layer have different energies. The respective flow impedances for each of these simulations are listed in Table 1. Note, the flow impedances are significantly lower than the vacuum impedance due to flow current, and the increased flow current seen in positive polarity simulations results in an undermatched MITL with respect to the effective machine impedance of 20.4 Ω [3].

For this reduced-power, self-limited flow case in negative polarity with no cell emission, the Mercury MIVA runs at 5.5 MV and 250 kA. In positive polarity, the line runs at 5.3 MV and 310 kA. The addition of

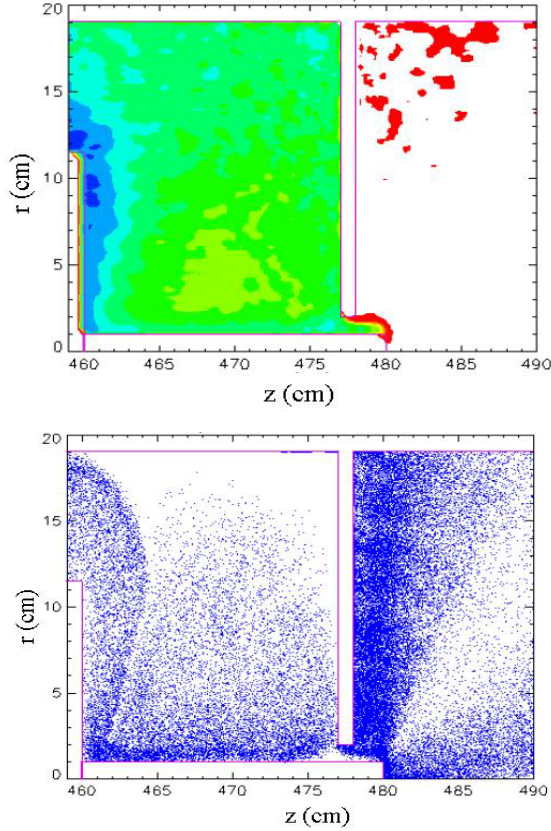


Figure 3. Positive polarity rod-pinch simulation results at 50 ns, showing current-enclosed contours (top) and electron positions (bottom). Each contour represents 25 kA of current flowing.

cell-emission in negative polarity increases the total current by about 5 kA. Thus, the self-limited flow impedance is polarity-dependent, and may depend on how the flow is established.

III. ROD-PINCH DIODE FOR MERCURY

In order to design a rod-pinch diode suitable for the front-end of Mercury, one must decide whether to use all of the current of the machine ($Z_{RP} \sim 20 \Omega$) or opt for a more standard [7], albeit higher-impedance rod-pinch diode ($Z_{RP} \sim 40\text{-}60 \Omega$), where Z_{RP} is the rod-pinch-diode impedance. In this work, we limit the scope to simply attempting to design a low-impedance rod-pinch diode in the hope of capturing all of the flow current into the diode.

The rod-pinch diode classically operates in the magnetically limited regime, with impedance given by

$$Z_{RP} = \frac{60}{\alpha} \sqrt{\frac{\gamma-1}{\gamma+1}} \ln\left(\frac{r_C}{r_A}\right) \quad (3)$$

where $\alpha \sim 2$. For numerical efficacy in this initial simulation series, the anode rod radius was chosen to be

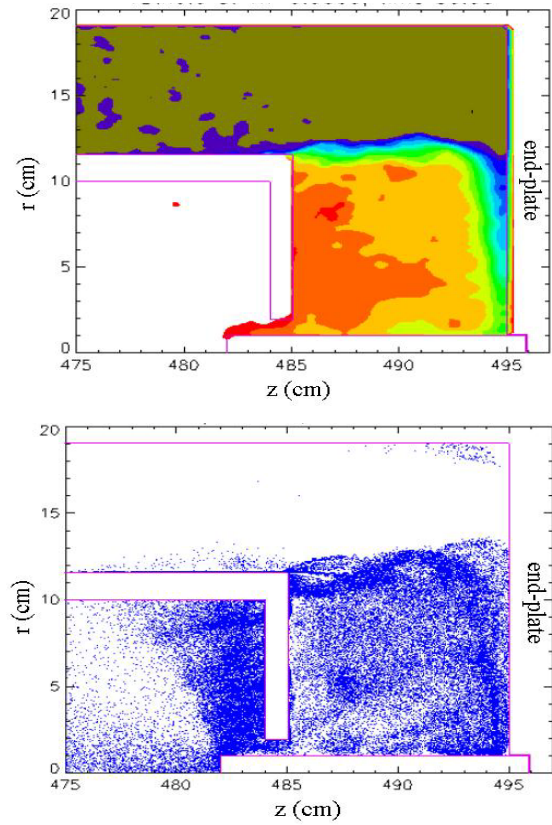


Figure 4. Negative polarity rod-pinch simulation results at 50 ns, showing current-enclosed contours (top) and electron positions (bottom). Each contour represents 25 kA of current flowing.

$r_A = 1$ cm, which is much larger than that typically used in radiography experiments [7,9]. Because the impedance is determined solely by the anode-to-cathode ratio in Eq. (3), $r_C = 2$ cm yields a 19Ω impedance between $V = 5 - 6$ MV. This diode geometry is used in the simulations described below in order to gain experience with coupling a diode with Mercury.

A. Positive Polarity Rod-Pinch Diode

Current-enclosed contours and electron positions at $t = 50$ ns from a simulation of a positive-polarity rod-pinch driven by the Mercury MIVA are shown in Fig. 3. In this simulation, the 23-cm-diameter center conductor is truncated abruptly at 460 cm, and a 20-cm long, 2-cm diameter anode rod is attached. The cathode extends downward radially from the outer conductor, thereby forming the rod-pinch diode. Proton-emission was allowed along the anode rod between $475 < z[\text{cm}] < 480$. The current-contours show that about 187 kA is running through the diode. About 63 kA of the flow current is lost upstream of the diode along the rod length, as shown in the electron plots and about 60 kA is lost to the anode upstream of the abrupt radial transition of the anode at $z = 460$ cm. The machine voltage and current at 50 ns is 5 MV and 310 kA, giving an effective total load impedance of 16Ω .

B. Negative Polarity Rod-Pinch Diode

Current-enclosed contours and electron positions from a simulation of a negative-polarity rod-pinch driven by the Mercury MIVA are shown in Fig. 4. In this simulation, the 23-cm-diameter center conductor is truncated abruptly at 485 cm and extended radially downward to serve as the cathode. A 12-cm-long, 2-cm-diameter anode rod is attached to the outer conductor at the axis of the machine and extended through a cathode hole, thereby forming the rod-pinch diode. Proton-emission was allowed along the anode rod between $482 < z[\text{cm}] < 495$. Only about 100 kA flows into the rod-pinch diode, with about 280 kA being lost to the end-plate of the machine (see Fig. 4). The machine impedance collapsed after 40 ns as the voltage dropped from 4 MV to 1 MV and the current rose from 200 kA to 380 kA. At 50 ns, the effective total load impedance was just 2.6 Ω . It is conjectured that the rod-pinch diode severely loads down the machine due to the large ion-emission surface along the 12-cm-long anode rod. In this geometry, the rod-pinch diode does not initially draw enough current to fully-insulate the MITL flow and prevent electron bombardment along the full length of the rod, subsequently leading to large regions of ion turn-on.

Note in these initial simulations, to assure the rod-pinch quickly transitioned into the magnetically limited phase, the anode rod initiated the emission of ions (protons) after exceeding a very low ion turn-on threshold. Further design studies of negative polarity rod-pinch diodes should use a more physically realistic ion turn-on threshold to prevent anomalously large ion currents.

IV. SUMMARY

PIC simulations of the electron power flow in the Mercury MIVA have been performed to investigate the electron power flow within the MITL, driven by the Mercury MIVA in both positive and negative polarities. Reduced-power simulations of the MIVA driving an open-circuit load demonstrate self-limited flow in positive polarity at 5.3 MV, 310 kA, with an 18- Ω flow impedance; conversely, the same load in negative polarity runs at 5.5 MV, 250 kA, with a 26- Ω flow impedance.

Low-impedance rod-pinch diode designs intended to couple all of the current from the Mercury MIVA were somewhat successful. In positive polarity, almost 200 kA at 5 MV was deposited into the anode rod. However, in negative polarity, excessive ion emission pulled down the impedance of the machine and severely undermatched the rod-pinch diode to the MIVA.

In both cases, the electron flow current that remained decoupled from the rod-pinch diode hit anode surfaces at large radii; these extraneous flows need to be controlled

in order to field a diode for radiographic purposes. Novel designs [8] for the rod-pinch in negative polarity may be required. Alternatively, unique designs that benignly shed excess current (in the form of a parallel load) or bifurcate the front-end into several parallel rod-pinch diodes may be utilized.

V. REFERENCES

- [1] P. Hoppe, J. Singer, H. Bluhm, K. Leber, D. Rusch, and Otto Stoltz, "Energy Balance Of The TW Pulsed Power Generator KALIF-HELIA," Proc. 13th Intl. Pulsed Power Conf., Las Vegas, NV, June 17-22, 2001, pp. 596-599.
- [2] R.J. Commisso, R.J. Allen, G. Cooperstein, R.C. Fisher, D.D. Hinshelwood, D.P. Murphy, J.M. Neri, P.F. Ottinger, D.G. Phipps, J.W. Schumer, O. Stoltz, K. Childers, V. Bailey, D. Creeley, J. Kishi, H. Nishimoto, I. Smith, P. Hoppe, and H.J. Bluhm, "Status Of The Mercury Pulsed Power Generator, A 6-MV, 360-kA Magnetically-Insulated Inductive Voltage Adder," these proceedings.
- [3] R.J. Allen, P.F. Ottinger, R.J. Commisso, J.W. Schumer, P. Hoppe, and I. Smith, "Electrical Modeling Of Mercury For Optimal Machine Design And Performance Estimation," these proceedings.
- [4] P.F. Ottinger, J.W. Schumer, R.J. Allen, R.J. Commisso, "Modeling Magnetically-Insulated Power Flow In Mercury," these proceedings, and references within.
- [5] B. Goplen, L. Ludeking, D. Smithe, and G. Warren, "User configurable MAGIC for electromagnetic PIC calculations," Comput. Phys. Commun. **87**, 54, 1995.
- [6] D.R. Welch, D.V. Rose, B.V. Oliver, and R.E. Clark, "Simulation techniques for heavy ion fusion chamber transport," Nucl. Instrum. Methods Phys. Res. A **464**, 134, 2001.
- [7] G. Cooperstein, J.R. Boller, R.J. Commisso, D.D. Hinshelwood, D. Mosher, P.F. Ottinger, J.W. Schumer, S.J. Stephanakis, S.B. Swanekamp, B.V. Weber, and F.C. Young, "Theoretical modeling and experimental characterization of a rod-pinch diode," Phys. Plasma **8**, 4618, 2001.
- [8] G. Cooperstein, S.B. Swanekamp, J.W. Schumer, P.F. Ottinger, R.J. Commisso, "Considerations of Rod-Pinch Diode Operation in Negative Polarity for Radiography," these proceedings.
- [9] R.J. Commisso, G. Cooperstein, D.D. Hinshelwood, D. Mosher, P.F. Ottinger, S.J. Stephanakis, S.B. Swanekamp, B.V. Weber, and F.C. Young, "Experimental Evaluation of a Megavolt Rod-Pinch Diode as a Radiography Source," IEEE Trans. Plasma Sci. **30**, pp. 338-351, Feb. 2002.
- [10] D.D. Hinshelwood, "BERTHA - A Versatile Transmission Line and Circuit Code," NRL Memorandum Report 5185, November 1983.